Kinetics of Contractile Activation in Voltage Clamped Frog Skeletal Muscle Fibers

Péter Szentesi, Zoltán Papp, Géza Szűcs, László Kovács, and László Csernoch
Department of Physiology, University Medical School Debrecen, Debrecen, Hungary H-4012

ABSTRACT Excitation-contraction coupling events leading to the onset of contraction were studied in single skeletal frog muscle fibers. This entailed the simultaneous measurement of the changes in intracellular calcium concentration using antipyrylazo III and fura-2, isometric force, and clamp voltage in a modified single vaseline gap chamber for the first time. The calcium transients were incorporated into an analysis of calcium binding to regulatory sites of troponin C (TnC) that permitted both a linear and a cooperative interaction. The analysis assumed that the onset of mechanical activation corresponds with a particular TnC saturation with calcium setting constraints for the calcium binding parameters of the regulatory sites. Using a simple model that successfully reproduced both the time course and the relative amplitudes of the measured isometric force transients over a wide membrane potential range, k_{off} of TnC was calculated to be 78 s^{-1} for the cooperative model at 10°C. Together with the above constraints this gave a dissociation constant of 8.8 ± 2.5 μM and a relative TnC saturation at the threshold (S_{th}) that would cause just detectable movement of 0.17 ± 0.03 (n = 13; mean ± SE). The predictions were found to be independent of the history of calcium binding to the regulatory sites. The observed delay between reaching S_{th} and the onset of fiber movement (8.7 ± 1.0 ms; mean ± SE, n = 37; from seven fibers) was independent of the membrane potential giving an upper estimate for the delay in myofilament activation. We thus emerge with quantitative values for the calcium binding to the regulatory sites on TnC under maintained structural conditions close to those in vivo.

INTRODUCTION

Excitation-contraction coupling in skeletal muscle, initiated by the application of a depolarizing step, can culminate in the appearance of a just-detectable muscle contraction. The required size of such depolarization depends on pulse duration. Adrian et al. (1969) explained such a strength-duration relationship in terms of the buildup of a hypothetical activator to a critical level for each such pulse. Horowicz and Schneider (1981) subsequently associated threshold contraction with a fixed transfer of intramembrane charge independent of the size and duration of the clamp pulse, and thus equated the proposed activator with the intramembrane charge movement. Melzer et al. (1986b), on the other hand, equated a critical amount of charge to the just-detectable release of calcium from the sarcoplasmic reticulum (SR). Intramembrane charge being the proposed activator was questioned by Miledi and co-workers (1983) who suggested the equality of the intracellular calcium concentration ($[Ca^{2+}]_i$) at the just-detectable contraction.

However, Kovács et al. (1987) demonstrated that the calcium transients associated with the onset of just-detectable movement depended on the size and duration of the depolarizing pulse. They proposed instead that different points on the strength-duration curve for the contraction threshold corresponded to equal occupancies of the regulatory sites of troponin C (TnC) by calcium.

The present work goes on to analyze the experimental strength-duration curve within the framework of a hypothesis that the onset of contraction depends upon a critical occupancy of the regulatory sites on TnC. The analysis examined whether this hypothesis would lead to an internally consistent description of the calcium binding to TnC. It also tested whether this simple assumption would allow the determination of the parameters of calcium binding to this regulatory protein. Although the presence of a threshold saturation, as will be shown, did set constraints for these parameters, their exact value could not be determined based solely on this assumption. An independent estimation had, therefore, to be introduced for one of the parameters by measuring and then fitting the force transients using a simple model of actomyosin interaction.

The analysis emerged with values for the calcium binding properties, and with a fixed value of the threshold occupancy of the regulatory sites on TnC in conditions close to in vivo and maintained filament structure. These values agree with earlier biochemical data and the independent analysis of Kovács et al. (1987). The measurements also revealed an ~9 ms difference between the calcium binding to TnC and the actual shortening, giving an upper estimate for the time necessary for the conformational changes and interactions within the contractile filaments.

Preliminary accounts on parts of this work have previously been published (Csernoch et al., 1994; Kovács et al., 1995).

Received for publication 21 October 1996 and in final form 18 June 1997.

Address reprint requests to László Csernoch, Department of Physiology, University Medical School Debrecen, Debrecen, P.O. Box 22, Hungary H-4012. Tel.: (36)-52-416-634; Fax: (36)-52-432-289; E-mail: CSL@PHYS.DOTE.HU

0006-3495/97/10/1999/13 $2.00

METHODS

Preparation and solutions

The frogs (*Rana esculenta*) were killed by rapid decapitation, followed by pithing. The dissection of single skeletal muscle fibers from the semiten-

dinosus muscles and the mounting of single fibers in a single vaseline-gap voltage clamp were done as described earlier in detail (Kovács et al., 1987). Briefly, the mechanical separation of fibers was carried out in Ringer's solution (in mM, 115 NaCl, 2.5 KCl, 1.8 $CaCl_2$, and 1 Tris sodium maleate) and the fiber was then transferred to the recording chamber. After completing the vaseline isolation the fiber segment in the open-end pool was permeabilized by applying a solution containing 0.01% saponin for 30 s. This solution was then exchanged to an internal solution containing, in mM, 102.5 Cs-glutamate, 5.5 $MgCl_2$, 5 Na_2ATP, 6 glucose, 5 creatine phosphate, 17.7 Tris maleate, 0.0082 $CaCl_2$, and 0.1 EGTA. The solution in the closed-end pool was exchanged to an external solution (in mM) 125 TEA-CH_3SO_3 (tetraethylammonium methanesulfonate), 5 Cs-HEPES, 2 $CaCl_2$, and 10^{-7} g/l TTX. All solutions were pH = 7.00 ± 0.05. The dyes antipyrylazo III (APIII) and fura-2 were applied in the internal solution in 1 mM and 50 μM concentration, respectively. Fura-2 was purchased from Molecular Probes, Inc. (Eugene, OR), and APIII from ICN Biochemicals, Inc. (Cleveland, OH); all other reagents were of analytical grade.

Fibers were connected to the force transducer with metal clips attached to the tendon. The sarcomere length was 2.0 − 2.4 μm as measured by ocular micrometer at 600× magnification. Although the contractions studied in this paper can be regarded as close to isometric, strong depolarization did cause the fibers to shorten by stretching the tendon (fibers seemed to be held fast at the cut end so contraction did not pull fiber portions out of the vaseline seal). Optical detection of tendon displacement (see below) revealed that these changes in fiber length were <5%. The measurements were carried out at low (8–11°C) temperatures to reproduce the experimental conditions in earlier studies (Adrian et al., 1969) and to enable the characterization of rapid events.

Experimental set-up

Fibers were voltage clamped as described earlier (Kovács et al., 1987) and the holding potential was set to −100 mV in all cases. The optical set-up was essentially the same as described in detail elsewhere (Klein et al., 1988; Sárközi et al., 1996). In brief, the experimental chamber was placed on the optical bench of an upright microscope and transilluminated using a tungsten halogen light source. The fiber was also epi-illuminated at 380 or 358 nm using a 75 W xenon arch lamp (Oriel 60000; Stratford, CT). The transmitted light intensities were measured at 720 and 850 nm using interference filters (Omega Opticals, U.S.A.) with 20 nm bandwidth while the fluorescence of fura-2 was detected at 510 nm using an interference filter (Omega Opticals, U.S.A.) with a bandwidth of 40 nm. Force development was measured using an AE801 force transducer (SensoNor, Horten, Norway) coated with silicon rubber to ensure electric isolation.

Data were acquired simultaneously on six channels (current, voltage, light intensities at 510, 720, and 850 nm, and force) using an online-connected computer. The analog to digital conversion was done on 12 bits at every 250 μs. Four consecutive points were averaged to yield the corresponding data point for every ms.

Calculation of the APIII calcium transients and the saturation of fura-2

Changes in intracellular free calcium concentration below the contraction threshold were calculated from the APIII and intrinsic fiber absorbance measured at 720 and 850 nm, respectively, as described earlier (Melzer et al., 1986a) using the kinetic correction (Csernoch et al., 1991). For suprathreshold depolarizations (see Results) composite calcium transients, calculated from APIII absorbance and fura-2 fluorescence, were used (Sárközi et al., 1996).

To calculate the relative saturation of fura-2 with calcium (S_f = [Ca-fura-2]/[fura-2]$_T$, where [Ca-fura-2] denotes the calcium bound to fura-2 while [fura-2]$_T$ the total fura-2 present) we followed the method described by Klein et al. (1988) and Csernoch et al. (1993). The fluorescence intensity was measured at 380 nm (F_{380}) during the pulse while the fluorescence intensity using 358 nm (F_{358}) as the incident light was linearly extrapolated from measurements done between pulses. The S_f was then calculated from

$$S_f = (R - R_{min})/(R_{max} - R_{min}) \quad (1)$$

where R denotes F_{380}/F_{358}, while R_{max} and R_{min} are the maximal and minimal values of R. To determine the rate constants ($k_{on,f}$ and $k_{off,f}$) of the calcium fura-2 reaction the

$$dR/dt = k_{on,f} \cdot [Ca^{2+}]_i \cdot (R_{max} - R_{min}) - k_{off,f} \cdot (R - R_{min}) \quad (2)$$

differential equation was fitted using the calcium transient measured with APIII (Klein et al., 1988). This method gave a direct, and internally consistent, calibration of the fura-2 signal inside the muscle fiber. Rearranging Eq. 2 and solving for $[Ca^{2+}]_i$ allowed us to calculate the calcium concentration changes in contracting fibers using the parameters determined from subthreshold pulses.

It should be noted that both dyes have been reported to bind to myoplasmic constituents (Baylor et al., 1986; Konishi et al., 1988). This might change their calcium binding properties, rendering the magnitude of the calculated $[Ca^{2+}]_i$ inadequate. Although this influences the obtained k_{on} of TnC the other parameters are not affected (see Discussion).

Optical detection of fiber contraction

The contraction threshold was determined visually at 400× magnification as described by Kovács et al. (1987). The optical signal accompanying fiber shortening was dissected from the absorbance change measured at 850 nm where APIII has no absorbance.

The displacement of the tendon was measured according to Kovács et al. (1987). In brief, a small alufoil was attached to the tendon and the slit was positioned so that upon contraction the alufoil covers greater and greater areas of the slit. The resulting decrease in light intensity was taken as the representation of tendon displacement. The alufoil was long enough to allow the placing of the slit far to the side of the fiber so fiber portions never interfered with the measurements. Measuring the total light intensity using slits of different length enabled us to convert the optical data into actual displacement. It should be noted that the illumination of the slit was found to be homogenous; therefore, the changes in light intensity were linearly related to displacement (i.e., when $\Delta I/I$ was −0.01 the alufoil moved by 1% of the length of the slit).

Statistical analysis and curve fitting

All averages are expressed as mean ± standard error of the mean (SE). Statistical significance was calculated using Student's t-test. To assess the $[Ca^{2+}]_i$ dependence of peak force the Hill equation was used:

$$F = \frac{F_{max}}{1 + 10^{n \cdot (pCa - pCa_{50})}} \quad (3)$$

where F_{max} is the maximal force that the fiber can develop, pCa_{50} is the negative logarithm of calcium concentration at which half maximal force is measured, and n is the index of cooperativity. The voltage (V_m) dependence of peak force (F) was fitted with the following equation:

$$F = \frac{F_{max}}{1 + e^{-(V_m - V')/k}} \quad (4)$$

where F_{max} has the same meaning as above, V' is the voltage where half maximal force is achieved, and k is the slope factor. Curves were fitted using the least-squares algorithm of Nelder and Mead (Johnson and Faunt, 1992). Latencies were calculated by fitting straight lines to the data points before the change in the trace and examining the variance of the determined slope as described earlier (Close, 1981).

Theory

Calculation of thin filament activation

The calculation of the binding of calcium to different intracellular binding sites followed the method of Csernoch et al. (1993) assuming the main buffers to be parvalbumin and troponin C. Both proteins were assumed to have two high-affinity calcium-magnesium sites, with TnC also having two low-affinity, calcium-specific sites, the binding to which initiates contraction.

The calcium binding to the regulatory sites of TnC was assumed to follow a simple four state scheme (S1) where T(0, 0) and T(1, 1) denotes the sites when both are free or occupied by calcium, while T(1, 0) and T(0, 1) stand for site 1 or site 2 alone having calcium bound, respectively. The binding of the first calcium was assumed to increase the affinity for the second by a factor of 10 (cooperative binding). For comparison calculations were done with the same affinity for both sites (independent binding) as well. The relative saturation (S_t = [Ca-Tn]/$[Tn]_T$, where [Ca-Tn] denotes the concentration of calcium bound to both regulatory sites and $[Tn]_T$ the concentration of these sites) was then calculated by numerically integrating the differential equations resulting from S1.

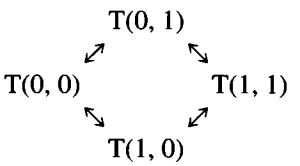

(S1)

When calcium was bound to the regulatory sites on a TnC molecule (calcium bound inhibited state) the adjacent tropomyosin was assumed to change its conformation to enable the actin and myosin interaction (calcium bound disinhibited state). These two states were assumed to be in instantaneous equilibrium. In the model this was manifested as an increase of the association rate of actin and myosin in the actomyosin model used (see below). Since neighboring tropomyosins were reported to interact (Wegner, 1979; Geeves and Lehrer, 1994) the probability that the activation of one will activate the next, even though its troponin C was free of Ca^{2+}, was also included.

The actomyosin interaction

A simple four state model (Scheme 2) was used to fit the measured force transients. Actomyosin was assumed to be either in the detached (1 and 2) or attached (3 and 4) state.

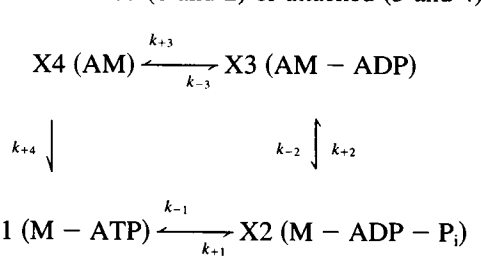

(S2)

To account for the activation by calcium the attachment rate of myosin to actin (k_{+2}) was increased 20× if the actin filament moved from the "calcium bound inhibited" to the "calcium bound disinhibited" state. To calculate the generated force first the differential equations resulting from S2

$$dX1/dt = -k_{+1} \cdot X1 + k_{-1} \cdot X2 + k_{+-4} \cdot X4, \quad (5a)$$

$$dX2/dt = k_{+1} \cdot X1 - (k_{-1} + k_{+2}) \cdot X2 + k_{-2} \cdot X3, \quad (5b)$$

$$dX3/dt = k_{+2} \cdot X2 - (k_{-2} + k_{+3}) \cdot X3 + k_{-3} \cdot X4, \quad (5c)$$

$$X1 + X2 + X3 + X4 = 1, \quad (5d)$$

where Xi are the relative occupancies in S2, k_{+i} and k_{-i} are the forward and backward rate constants, were solved. The force at time t ($F(t)$) was assumed to be proportional to the increase in attached states (ΔAS), that is,

$$F(t) = N \cdot \Delta AS, \quad (6)$$

where N is the proportionality coefficient (depends on the number of cross-bridges and on the force generated by a single cross-bridge) and ΔAS = {X3(t) + X4(t)} − {X3(t = 0) + X4(t = 0)}. To account for the increased affinity of calcium binding to TnC with attached cross-bridges (Güth and Potter, 1987) k_{off} was also varied proportionally with the attached states

$$k_{off}(t) = k_{off}(0)/\{1 + [(M - 1) \cdot \Delta AS/\Delta AS_{max}]\}, \quad (7)$$

where $k_{off}(0)$ is the rate at rest (t = 0), M is the relative change in affinity, and ΔAS_{max} is the maximal change in attached states.

Implementation of the model

A computer program written in PASCAL (Borland Pascal 7.0) implemented the model. This first analyzed the events at the contraction threshold and set the constrains for the binding properties of TnC, between k_{on} and k_{off} as well as between K_d and the threshold saturation, S_{th}, (see Results). Using a set of starting values (for calcium binding to TnC and those in Table 1) the program then determined the

TABLE 1 Parameters of the acto-myosin interaction used in the model calculations

Description	Value
Transition from X1 to X2 (k_{+1})	130 s^{-1} (1)
Transition from X2 to X1 (k_{-1})	12 s^{-1} (1)
Association constant of M to A	10^4 M^{-1} (2)
Transition from X3 to X2 (k_{-2})	—*
Transition from X3 to X4 (k_{+3})	8.3 s^{-1} (3)
Transition from X4 to X3 (k_{-3})	*
Detachment rate of M from A (k_{+4})	*

M, myosin; A, actin. Abbreviations used in the text are given in parentheses.

*Parameters varied in fits.

(1) Goldman, 1987; (2) Tregear and Marston, 1979; (3) Dantzig et al., 1992.

calcium binding to the regulatory sites on TnC. The calculation proceeded to determine the appearance of calcium bound disinhibited states using the relative calcium occupancy of TnC and S_{th}. This change induced the transition of the actin-myosin system from detached to attached states. At rest (before stimulation) 96% of actin and myosin were in the detached form, calculated as the steady-state solution with the parameters given in Table 1.

The calculated force transient ($F(t)$) was then compared to the measured. Using the method of Nelder and Mead (Johnson and Faunt, 1992) the parameters (k_{off}, M, k_{-2}, k_{-3}, and k_{+4}) were adjusted to obtain a least-squares fit. The fitting procedure usually included 3–5 calcium and force transients and 200–300 points from each trace. It gave chi-squared (χ^2) values in the range of 0.001–0.005 if χ^2 was normalized to the number of points and to the maximal attained force.

RESULTS

The Results are organized into three sections. The first section examines the events at different points of the strength-duration curve for just-detectable contraction. It concludes showing that, although a clear relationship can be established between the different parameters of calcium binding to TnC, they cannot be determined without additional information. The second describes the simultaneous measurement of events in excitation-contraction coupling, changes in $[Ca^{2+}]_i$ and force, in a single vaseline gap system under voltage clamp control. The third section brings together the results from the previous two using a simple model to fit the force transients on the basis of the measured $[Ca^{2+}]_i$ to emerge with values for the calcium binding properties of TnC.

Analysis of threshold events

Calcium binding properties of troponin C

When a skeletal muscle fiber is depolarized the increase in $[Ca^{2+}]_i$ has to exceed certain levels before contraction will occur. Depending on the length and amplitude of the depolarizing pulse this attained $[Ca^{2+}]_i$ might vary. To account for this observation we assumed, following the line of reasoning by Kovács et al. (1987), that the saturation of TnC has reached a certain critical level (threshold saturation, S_{th}) before just-detectable contraction occurred. In the following we first test whether this assumption would lead to a single set of parameters describing the calcium binding to TnC.

In the experiment presented in Fig. 1, calcium transients were recorded at two points of the strength-duration curve for just-detectable contraction, namely at pulse durations of 10 and 100 ms, respectively. Fig. 1, *A* and *B* show the corresponding APIII calcium transients while *C* and *D* present the saturation of fura-2 calculated from the measured fluorescence. In accordance with the findings of Kovács et al. (1987), the shorter pulse brought about the

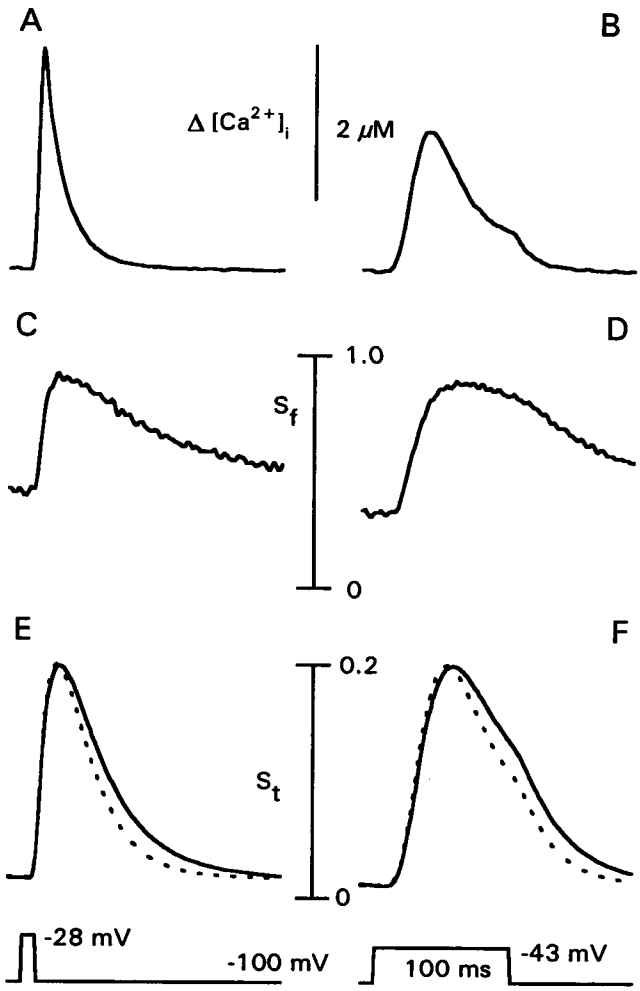

FIGURE 1 Changes in the intracellular free $[Ca^{2+}]$ (*A* and *B*) and in the relative saturation of fura-2 (*C* and *D*) and of troponin C (*E* and *F*) at two different pulses of the strength-duration curve for just-detectable movement. The pulses were a 10 ms depolarization to −28 mV and a 100 ms depolarization to −43 mV for the left and right columns, respectively. The change in membrane potential is shown as the lowermost traces. The rate constants for the calcium binding to TnC were selected so that the maximal saturation would reach 0.2. The values were $k_{on} = 0.84 \times 10^7\ M^{-1}\ s^{-1}$ and $k_{off} = 85.9\ s^{-1}$ for the binding of the first calcium in the cooperative model, solid traces, and $k_{on} = 1.18 \times 10^7\ M^{-1}\ s^{-1}$ and $k_{off} = 76.2\ s^{-1}$ for the independent binding model, dotted traces. Fiber 75, [APIII] = 628 and 641 μM, [fura-2] = 21.5 and 22.1 μM for the left and right columns, respectively; pl = 105 μm, d = 104 μm, sl = 2.0 μm, T = 9.1°C.

greater increase in $[Ca^{2+}]_i$, 2.9 and 1.8 μM for the 10 and 100 ms pulse, respectively, in spite of the fact that they both resulted in the same mechanical activation. In the 13 fibers included in this study these values were 2.40 ± 0.24 and 1.53 ± 0.18 μM, respectively, the former being higher in each and every experiment.

As an example, Fig. 1, *E* and *F* show that the rate constants of calcium binding to TnC can be selected so that the calcium bound to TnC will reach the same critical level (0.2 in this example) for both the 10 (Fig. 1 *E*) and 100 ms (Fig. 1 *F*) pulse. The attained maximum of saturation, 0.2, cor-

responds to S_{th} since the increase in $[Ca^{2+}]_i$ resulted in a just-detectable movement. It is also demonstrated that this selection can be made using either the cooperative (*solid traces*) or the independent (*dotted traces*) binding model for the calcium-TnC reaction. The rate constants used in the calculations were $k_{on} = 1.18 \times 10^7$ and 0.84×10^7 M^{-1} s^{-1}, whereas $k_{off} = 76.2$ and 85.9 s^{-1} for the independent and cooperative models, respectively. It should be noted that this selection of the rate constants was unique for the particular S_{th}. Suitable k_{on}–k_{off} pairs, however, as will be shown in Fig. 2 *A* and *B*, were to be found not only for $S_{th} = 0.2$, but for any depicted saturation as well.

As shown in the figure (Fig. 1, *E* and *F*) the kinetics of the calcium bound to TnC, especially the rising phases, were almost completely independent of the model chosen. The only difference seen was a shift in the declining phase of the transients calculated with the cooperative model. It has to be noted that this similarity in time courses of the calculated calcium binding changed very little with changing the desired final saturation (data not shown). Nevertheless, increasing the maximal saturation did result in an increase of the rate of rise during and in a slowing down of the decay after the depolarizing pulse. As an indication of the similar time courses during the rising phase, the time-to-peak of calcium bound to TnC varied little with the model used, being 58 and 28 ms with the cooperative, while 51 and 24 ms with the independent model for the 100 and 10 ms pulses, respectively. Furthermore, changing the maximal saturation from 0.1 to 0.9, the time-to-peak shifted by only 2 ms, that is, from 58 to 56 ms for the 100 ms pulse and from 28 to 27 ms for the 10 ms pulse in the cooperative model. In all fibers studied the time-to-peak saturation of TnC was similarly independent of the actual value of the maximum (data not shown).

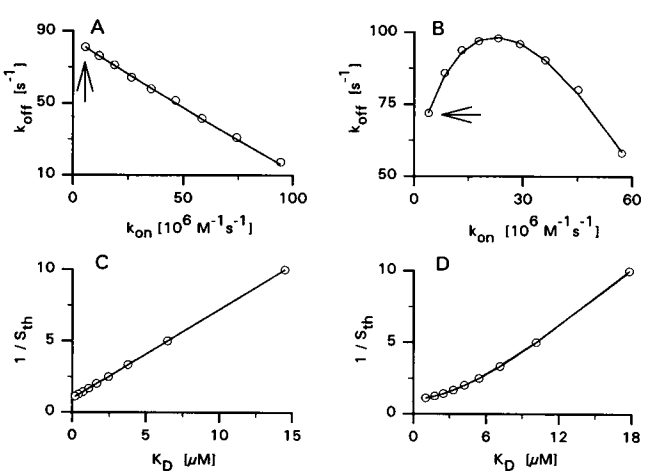

FIGURE 2 Determination of the parameters in the calcium troponin C reaction. Panels *A* and *C* show the case of independent binding while *B* and *D* present values obtained with the cooperative model. (*A* and *B*) Corresponding values of k_{on} and k_{off} rate constants that gave equal maximal saturation ($S_t = 0.1, 0.2, \ldots, 0.9$) for the calcium transients in Fig. 1, *A* and *B*. Points corresponding to $S_t = 0.1$ are marked with arrows. (*C* and *D*) The reciprocal of the maximal saturation versus the dissociation constant calculated from the corresponding points in *A* and *B*. The solid lines in *C* and *D* show the least squares fit of Eqs. 9a and b to the data with $[Ca^{2+}]_i(t_m) = 1.48$ and 1.24 μM and *y* intercepts of 0.97 and 0.91, respectively. Same fiber as in Fig. 1.

Carrying out the above analysis for $S_{th} = 0.1, 0.2, \ldots, 0.9$ we determined those k_{on}–k_{off} pairs that gave equal peak saturation for the calcium transients in Fig. 1, *A* and *B*. These values, k_{off} versus k_{on}, are plotted in Fig. 2, *A* and *B* for the independent and cooperative models, respectively. The graphs demonstrate that the selection of k_{on} and the corresponding k_{off} was not arbitrary for any given saturation using either the independent (Fig. 2 *A*) or the cooperative (Fig. 2 *B*) model. On the contrary, only one such pair was to be found for each and every saturation.

To demonstrate the dependence of the rate constants on the given saturation, let t_m denote the time when TnC reaches its maximal saturation (if the pulse caused just-detectable contraction this saturation is S_{th}). For a single independent binding site it then follows that at time t_m, when $d(S_t)/dt = 0$,

$$k_{on} \cdot [Ca^{2+}]_i(t_m) \cdot (1 - S_{th}) = k_{off} \cdot S_{th}, \tag{8}$$

where $[Ca^{2+}]_i(t_m)$ denotes the calcium concentration measured at time t_m. Solving Eq. 8 for $1/S_{th}$ yields

$$1/S_{th} = 1 + K_D/[Ca^{2+}]_i(t_m) \tag{9a}$$

where K_D is the dissociation constant for TnC. Following the same line of reasoning with the cooperative model yields

$$\frac{1}{S_{th}} = 1 + \frac{K_D}{[Ca^{2+}]_i(t_m)} \cdot \frac{K_D + [Ca^{2+}]_i(t_m)}{K_D + A_f \cdot [Ca^{2+}]_i(t_m)}, \tag{9b}$$

where A_f is the factor by which the affinity of the second site changes when the first binds calcium, and all other parameters are the same as before. Since t_m was found to be essentially independent of S_t (see above), Eqs. 9a and 9b predict a simple relationship between the dissociation constant and the reciprocal of the relative saturation at the contraction threshold.

Fig. 2, *C* and *D* present $1/S_{th}$ as a function of the calculated K_D using the values from Fig. 2, *A* and *B*, respectively, the solid lines are the least squares fits of Eqs. 9a and b to the data points. In accordance with the equations, the *y* axis intercept was close to unity in all cases studied, for both the independent and the cooperative model, averaging 1.01 ± 0.02 ($n = 13$).

Note that the relationships presented in Fig. 2 are not enough to determine all parameters of calcium binding to TnC. Nevertheless, they do set constraints and, furthermore, if any one of k_{on}, k_{off}, and S_{th} is determined independently the other parameters can be calculated directly from these relationships. To obtain this independent determination in the following sections of Results we will introduce the simultaneous measurement of $[Ca^{2+}]_i$ and force and then fit the measured force transient using a simple model.

This fit enabled us to determine the dissociation rate of calcium from TnC yielding an average k_{off} of 78 s^{-1} for the cooperative, and 56 s^{-1} for the independent models, respectively (see Table 2 and related text). Using the cooperative model and this fitted value for k_{off} the corresponding k_{on} was 0.69×10^7 M^{-1} s^{-1} for the fiber presented in Figs. 1 and 2. This resulted in a K_D = 11.3 μM and a threshold saturation of 0.19. On average for the 13 fibers studied $k_{on} = 0.89 \pm 0.25 \times 10^7$ M^{-1} s^{-1}, $K_D = 8.8 \pm 2.5$ μM and the threshold saturation was 0.168 ± 0.031 with the cooperative model using k_{off} obtained from the fitting of force transients.

The threshold saturation of TnC is independent of changes in the resting $[Ca^{2+}]_i$

An increase in the resting calcium concentration would result in a corresponding increase in the resting saturation of the regulatory sites on TnC. If a threshold saturation does exist, such an increased resting saturation should decrease the amplitude of the calcium transients required to evoke a just-detectable contraction. Fig. 3 demonstrates that this is indeed what was observed. Resting $[Ca^{2+}]_i$ was therefore varied and the calcium transients corresponding to points on the strength-duration curve were analyzed to provide an independent test of the presence of a threshold saturation.

The fiber was held at a holding potential of −100 mV and the analysis presented in connection with Figs. 1 and 2 was carried out. The trace in Fig. 3 *A* shows the APIII calcium transient corresponding to the 100 ms pulse of the strength-duration curve while the trace in *D* demonstrates the calculated calcium binding to TnC. The rate constants used in the calculation were $k_{on} = 0.47 \times 10^7$ M^{-1} s^{-1} and k_{off} = 78 s^{-1}. Two interventions were then used to change the resting $[Ca^{2+}]_i$, namely, a subthreshold prepulse from the −100 mV holding potential to −57.2 mV (Fig. 3 *C*) that resulted in a 327 nM increase in $[Ca^{2+}]_i$ and the lowering of the holding potential to −80 mV (Fig. 3 *B*), resulting in a 84 nM increase in the resting $[Ca^{2+}]_i$.

The upper row in Fig. 3 shows the APIII calcium transients for the 100 ms pulses of the strength-duration curve corresponding to the above interventions. The figure demonstrates that the higher the resting $[Ca^{2+}]_i$ and the consequent increase in the saturation of TnC before the pulse were, the smaller the amplitude of the calcium transients became. This decrease was likely due to the change in resting $[Ca^{2+}]_i$ rather than to changes in fiber status, since the sequence of obtaining the records was *A*, *C*, and finally *B*.

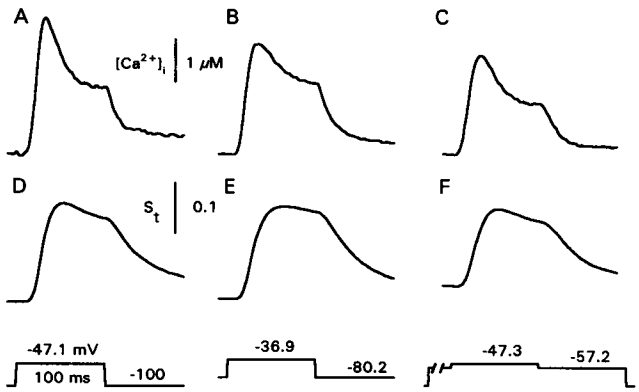

FIGURE 3 The effect of resting $[Ca^{2+}]_i$ on the calcium transients measured at the contraction threshold (*A*, *B*, *C*) and on the calculated calcium binding to TnC (*D*, *E*, *F*). In order to change the resting $[Ca^{2+}]_i$ compared to control (*A* and *D*) the fiber was either depolarized to −57.2 mV (threshold of just-detectable calcium release) for 100 ms (*C* and *F*) or its holding potential was decreased to −80 mV (*B* and *E*). The changes in membrane potential are given below the records. The rate constants of the calcium TnC reaction were then determined for the transient in *A* (k_{on} = 0.47×10^7 M^{-1} s^{-1} and 78 s^{-1}; for details see text) and used for all traces in the figure. The resting $[Ca^{2+}]_i$ were 128, 212, and 455 nM, as determined from the fura-2 saturations before the pulse, for the traces in *A*, *B* and *C*, respectively. Fiber 97, [APIII] = 410–667 μM, [fura-2] = 41.3–42.6 μM, pl = 140 μm, d = 78 μm, sl = 2.0 μm, T = 8.5–9.7°C.

Using the rate constants from *A*, the saturation of TnC was calculated for the records with different resting $[Ca^{2+}]_i$. Taking the resting occupancy into account the maximal saturations reached for these pulses were almost identical, being 0.209, 0.204, and 0.199 for *D*, *E*, and *F*, respectively, showing that the selection of rate constants was close to independent of the resting calcium. There was a small decrease in maximal saturation with increasing resting $[Ca^{2+}]_i$ not only in this fiber but in all five fibers studied of the order of 1.1 ± 0.3% for a 200 nM increase in resting $[Ca^{2+}]_i$.

This observation shows that the calculated threshold saturation of TnC was close to independent of the resting saturation of TnC before the test pulse. It also establishes the fact that the parameters of calcium binding to TnC do not depend on previous history. It renders the possibility that diffusional delays would explain the inequality of the calcium transients corresponding to different points on the strength-duration curve for just-detectable contraction unlikely.

TABLE 2 Parameters of the acto-myosin interaction and calcium binding to TnC determined from the fits of composite calcium transients to the measured force

k_{off} (s^{-1})	Mean ± SE	k_{-2} (s^{-1})	k_{-3} (s^{-1})	k_{+4} (s^{-1})
77.9 ± 14.8*	3.6 ± 0.8*	19.1 ± 2.9	10.6 ± 3.0	24.6 ± 3.1
56.3 ± 11.2*	5.6 ± 1.0*	18.4 ± 2.7	15.4 ± 3.3	21.7 ± 3.6

Calcium binding to the regulatory sites of TnC used the cooperative model for the first, and independent binding for the second row. Values are mean ± SE from six fibers.
*Significantly ($p < 0.04$) different for the two binding models of TnC.

Simultaneous measurement of calcium concentration and force

The following section introduces how force and $[Ca^{2+}]_i$ can be measured in a single vaseline gap system. It demonstrates that the overall parameters, voltage- and $[Ca^{2+}]_i$-depen-

dence of force were not far from those in intact and skinned fibers, rendering the measured force transients suitable for the determination of the calcium binding properties of TnC. It also shows that, close to the threshold, force and optical signals have a similar time course.

Optically detected fiber displacement reflects the time course of measured force

When absorbance measurements are carried out on contracting fibers, a late component of light intensity change can be detected which has been associated with fiber displacement and termed movement artifact (e.g., Melzer et al., 1986a). Although this movement artifact was present at all wavelengths, the correction of the 720 nm signal with the 850 nm signal did not fully eliminate it. Fig. 4 *A* shows such a calcium transient, calculated from the signals obtained at 720 and 850 nm, superimposed on the measured force. The *early* increase in $[Ca^{2+}]_i$ that preceded the development of force can be regarded as good estimate of the actual time course of calcium concentration change, whereas the broad peak present after the pulse was most likely a movement artifact. For pulses that caused slightly suprathreshold contractions the time course of movement artifact and measured force agreed remarkably well (Fig. 4 *A*).

To calculate the time course of $[Ca^{2+}]_i$ devoid of movement artifacts composite calcium transients were constructed following the method of Sárközi et al. (1996). The composite calcium transient (Fig. 4 *B*) contained the APIII calcium signal at early times and the change in $[Ca^{2+}]_i$ calculated from the fura-2 fluorescence at later parts of the record. The transition in Fig. 4 *B* is marked by a horizontal line positioned on the composite calcium transient. It corresponded in time to the point where the APIII and fura-2 calcium transients started to deviate from each other, 9 ms after the termination of the pulse for the record in Fig. 4 *B*. As demonstrated in Fig. 4, and also in Figs. 5 and 8, such composite calcium transients were readily calculated from the absorbance and fluorescence records and provided a fair estimate of $[Ca^{2+}]_i$ in contracting fibers. The resulting time course of $[Ca^{2+}]_i$ and its relative position to the force transient resembled that measured on intact fibers with action potential stimulation (e.g. Claflin et al., 1994).

The simultaneous detection of fiber absorbance and force enabled us to correlate the components of light intensity change and fiber contraction. Fig. 4 *C* demonstrates that the displacement of the tendon, measured optically as the dis-

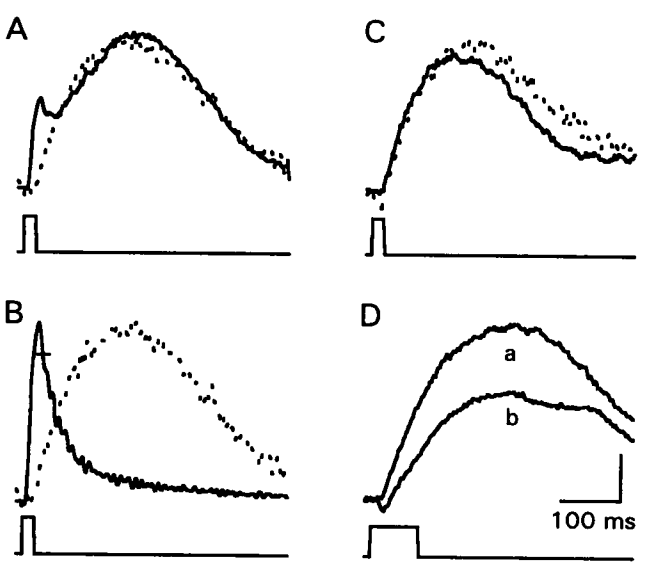

FIGURE 4 Comparison of the kinetics of the optical signals and the force transient. (*A*) Superimposed records of a calcium transient, calculated solely from the absorbance records, and changes in force (all force transients are dotted in the figure). Note that the early rise in $[Ca^{2+}]_i$ was followed by a secondary broad peak, the kinetics of which resembled the time course of the force transient. (*B*) Same as in *A* except the APIII calcium transient from *A* was replaced by the composite record. The horizontal tick marks the point from which $[Ca^{2+}]_i$ was calculated from the fura-2 signal. (*C*) Superimposed traces of force and the displacement of the tendon. Note that light intensity decrease is shown as upward deflection to ease the comparison. (*D*) Light intensity changes measured at 850 nm on the alufoil attached to the tendon (*trace a*) and on the fiber (*trace b*). The signal from the fiber showed two components from which the second started at the same time and had the same kinetics as the signal representing the displacement of the tendon. Fiber 214, the depolarizing pulse was to 0 mV for 20 ms (*A* and *C*) and to −20 mV for 80 ms (*B* and *D*). APIII concentration ([APIII]) = 387 for panel *C* and 432 μM for panel *D*; path length (*pl*) = 85 μm, horizontal diameter (*d*) = 80 μm, sarcomere length (*sl*) = 2.5 μm, temperature (*T*) = 10.7°C. Vertical calibration corresponds to 1 or 2 μM, 6 μN, and -10^{-3} (= 0.2 μm) for $[Ca^{2+}]_i$ (*A* or *B*), force and $\Delta I/I$, respectively.

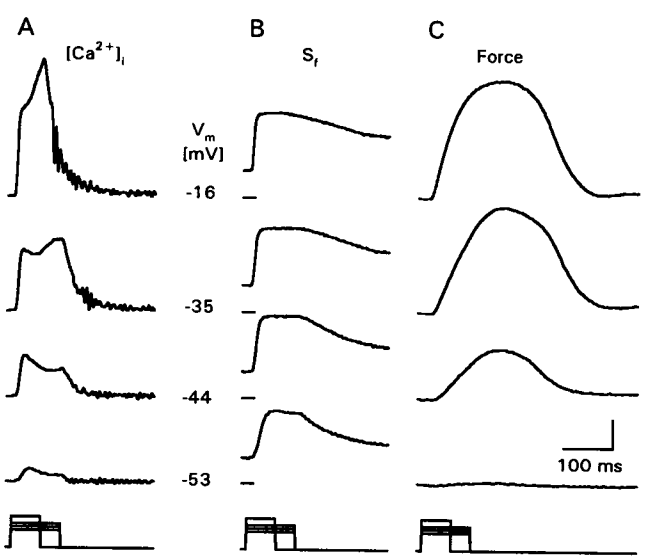

FIGURE 5 Voltage dependence of $[Ca^{2+}]_i$ and force increase. (*A*) Composite calcium transients calculated from the absorbance and fluorescence signals. (*B*) The relative saturation of fura-2, the horizontal ticks below each trace represent 0% saturation. (*C*) Simultaneously measured force. Note that there was a definite increase in $[Ca^{2+}]_i$ at the smallest depolarization without any sizable change in force. The time courses of membrane potential change are given below the records, the actual values during the test pulses are shown next to the traces in each row. Fiber 266, [APIII] = 780–828 μM, fura-2 concentration ([fura-2]) = 18.1–18.4 μM, *pl* = 105 μm, *d* = 78 μm, *sl* = 2.2 μm, *T* = 10.7°C. Vertical calibration corresponds to 2 μM, 0.3 and 75 μN for $[Ca^{2+}]_i$, S_f and force, respectively.

placement of an alufoil attached to it, and the measured force were almost identical in time course. This is expected if the elasticity of the connection between the force transducer and the actually contracting element is linear. If the same pulse was repeated with the slit of illumination positioned first on the alufoil (trace a in Fig. 4 *B*) and then on the fiber (trace b) the components of fiber absorbance could be clearly dissected. To exclude any interference from APIII, absorbance changes were measured at 850 nm. The early increase (downward deflection) in light intensity on trace b reflects the intrinsic absorbance change of the fiber (see Melzer et al., 1986a) and was always present even below the contraction threshold if calcium was released from the SR. Note that a longer pulse, at smaller depolarization, was used in this case where the intrinsic absorbance change of the fiber could be distinguished more readily. The intrinsic signal was interrupted by a decrease in light intensity, the time course of which followed closely the displacement of the tendon. Note how well the latencies of trace a and of the second component of trace b match. The calculated average difference for the latencies was <1 ms, the former being longer, for the 13 fibers with appropriate pulses. This latter component can, therefore, be taken as the optical representation of the time course of contraction in measurements where the slit was positioned on the fiber.

Pulses presented in Fig. 4 were only slightly suprathreshold, maximal force being 30 μN (<5% of maximal force; compare also to Figs. 5, 6, and 8), to demonstrate that optical signals were very sensitive to movement. Although the time course of the movement artifact cannot completely replace the actual force transient, the latency of the optical records is probably a better measure for the latency of contraction for small force increases due to the smaller noise on the optical signals.

Comparison of calcium and force transients

To compare $[Ca^{2+}]_i$ and force over a wide voltage range and, therefore, over a wide range of mechanical activation, composite records of calcium transients were calculated from the APIII absorbance and fura-2 fluorescence. Fig. 5 presents the composite calcium transients (Fig. 5 *A*), the calculated saturation of fura-2 (Fig. 5 *B*), and the measured force (Fig. 5 *C*). The depolarizations only went as far as −15.9 mV (lasting 60 ms), this does not represent full activation: larger contractions often damaged the vaseline seal. The composite calcium transients as well as the saturation of fura-2 in these contracting fibers showed all the features presented previously on non-contracting (stretched) fibers in a wide voltage range. During the course of all the experiments, the resting $[Ca^{2+}]_i$ remained almost constant, as could be assessed from the similar fura-2 saturations before each pulse.

With increasing depolarization, the maximal force not only became greater but also its rate of rise increased, and the latency of the transients decreased from 52 ms at −53.3 mV to 15 ms at −15.9 mV, in accordance with earlier voltage clamp measurements (Gomolla et al., 1983). Fig. 6 shows the voltage dependence of the maximal force (Fig. 6 *A*) for another fiber where several long, 80 or 100 ms, pulses were repeated to assess the voltage dependence more reliably. Fitting Eq. 4 to the data points (presented as a solid line in Fig. 6 *A*) revealed a steep voltage dependence: the slope factor was found to be 5.4 mV with $V' = -43.3$ mV and $F_{max} = 930$ μN.

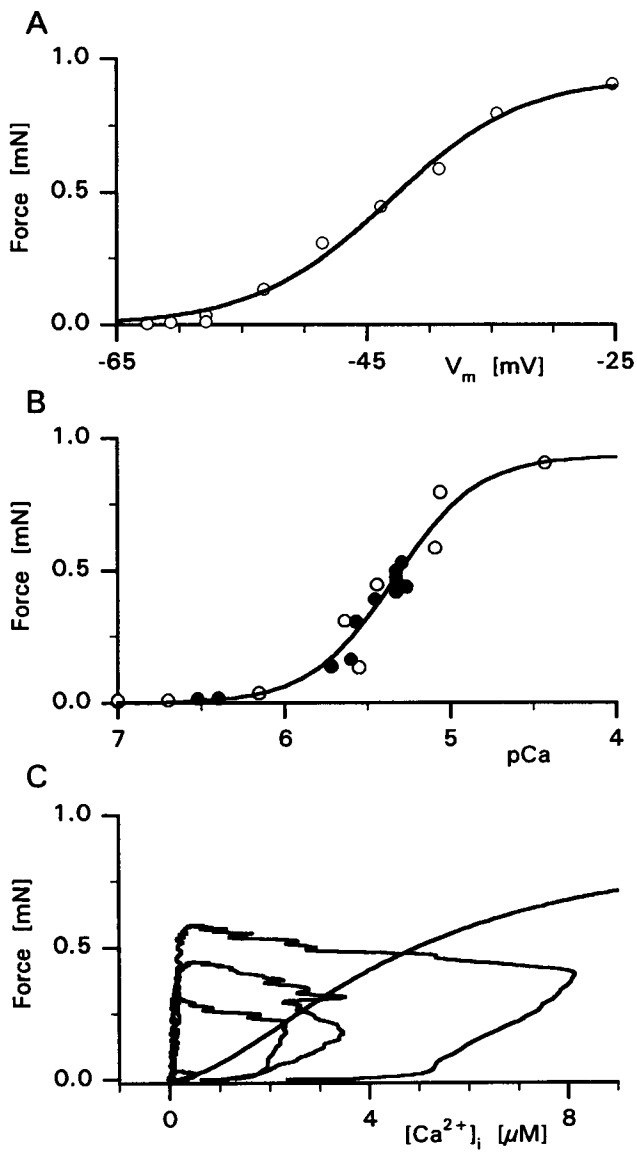

FIGURE 6 Voltage and $[Ca^{2+}]_i$ dependence of the parameters of the force transients. (*A*) Voltage dependence of peak force. Values taken from measurements where the duration of the test pulse was 80 or 100 ms. The solid line shows the least squares fit of Eq. 4 to the data points with F_{max} = 930 μN, $V' = -43.3$ mV, and $k = 5.4$ mV. (*B*) Calcium concentration dependence of peak force. The graph shows data from pulses with shorter durations (*filled circles*) as well. Least squares fit of Eq. 3 to the open symbols is superimposed as a solid line. The parameters of the fit were F_{max} = 933 μN, $pCa_{50} = 5.34$, $n = 1.73$. (*C*) Phase plots of four force transients. Superimposed is the fit from part B. Note that the scale of the abscissa is linear. Fiber 275, $sl = 2.4$ μm, $T = 10$°C.

To enable a comparison with skinned preparations Fig. 6 *B* presents the $[Ca^{2+}]_i$ dependence of the peak force. Note, however, that this comparison should be regarded as approximate since tetanic force could not be determined. Values from pulses of shorter duration, 20 to 60 ms, were also included into this graph (*filled symbols*). Data points representing the long pulses (*open symbols*) were fitted with the Hill equation, Eq. 3, resulting in F_{max} of 933 μN, pCa_{50} of 5.3, and the index of cooperativity of 1.73. In six fibers where sufficient numbers of long pulses were applied, F_{max} was 660 ± 94 μN (mean ± SE), pCa_{50} was 5.43 ± 0.09, and the index of cooperativity was 1.79 ± 0.11. These values represent a calcium dependence that was shifted to higher $[Ca^{2+}]_i$ and was less steep as compared to skinned fibers (e.g., Stienen et al., 1995). The difference might arise from the fact that the points, peak force versus peak $[Ca^{2+}]_i$, do not represent a steady state.

This possibility was tested by plotting the force-$[Ca^{2+}]_i$ relationship during four typical transients on the phase plane. As shown previously for cardiac cells (Dobrunz et al., 1995), the force versus $[Ca^{2+}]_i$ relationship was independent of the level of previous activation during relaxation. In cardiac cells, the calcium dependence of tetanic force followed the same curve as the relaxation process, while that of peak twitch force was shifted to higher $[Ca^{2+}]_i$. To demonstrate that this was the case for skeletal muscle fibers as well, the calcium dependence of peak force from Fig. 6 *B* was replotted in Fig. 6 *C* as a continuous curve. The position of the calculated calcium dependence of peak force relative to the phase plots in our measurements argues in favor of the hypothesis that part of the lower cooperativity and the higher pCa_{50} might arise from the non steady-state conditions during an 80–100 ms pulse.

These data suggest that the parameters of contractile activation in the single vaseline gap are not far from those of intact and skinned fibers; therefore, the cut fiber preparation should provide a convenient system for studying the kinetic relationship between $[Ca^{2+}]_i$ and force.

Kinetic analysis of force transients

Having established the measurement of force the following section aims at the determination of a depicted parameter, k_{off}, of calcium binding to TnC to complete the analysis of the calcium binding of this regulatory protein. We first demonstrate that, in line with expectations, there is a lag between calcium binding and force production, presumably due to the conformational changes taking place in the thin and thick filaments. This is followed by the fitting of the force transients with a simple model of actomyosin interaction to give k_{off} as one of the fitted parameters.

Comparison of calcium binding to TnC with optical signals above the contraction threshold

The composite calcium transients were used to calculate the calcium binding to TnC when the absorbance records were obscured with movement artifacts. The rate constants for the TnC reaction (k_{on} = 0.67 × 10^7 M^{-1} s^{-1}, k_{off} = 78 s^{-1}) were determined from the 10 and 100 ms long pulses of the strength duration curve as described previously. Fig. 7 *A* presents an example where the saturation of TnC with calcium was calculated at and above threshold. To minimize the effect of the voltage-dependent nature of the intrinsic

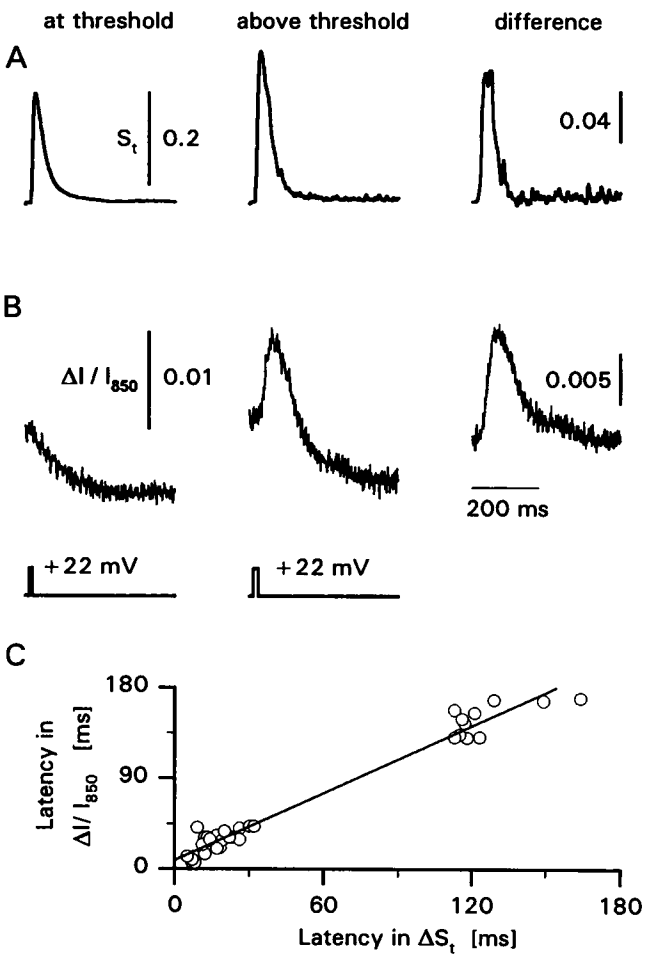

FIGURE 7 Comparison of the time courses of changes in the relative saturation of TnC and the optical representation of fiber shortening. (*A*) The saturation of TnC calculated from composite calcium transients (not shown), using the cooperative model with k_{on} = 0.67 × 10^7 M^{-1} s^{-1} and k_{off} = 78 s^{-1}, both at and above the threshold. Subtracting the trace at threshold from that above (Difference) the resulting excess calcium bound to TnC (ΔS_t) should be directly responsible for the shortening (see text for further details). The depolarization was to +22 mV for 10 ms and 15 ms at and above the threshold, respectively. (*B*) Simultaneously recorded changes in light intensity at 850 nm. The shortening of the fiber caused a transient upward deflection superimposed on the monotonic decay (increases in light intensity are shown as downward deflections) seen at threshold. The record shown under Difference is thus the optical representation of the time course of fiber movement. (*C*) The latency, measured from the start of the first depolarization, in $\Delta I/I_{850}$ plotted as a function of the latency in ΔS_t. The group of points with longer latencies (>100 ms) were calculated from depolarizations with prepulses. Fiber 95 for *A* and *B*; 7 fibers for *C*. [APIII] = 395 and 400 μM, [fura-2] = 31.9 and 32 μM for at and above threshold, respectively, *pl* = 105 μm, *d* = 80 μm, *sl* = 2.3 μm, *T* = 11.3°C.

fiber absorbance change, the suprathreshold pulse was evoked by increasing the duration of the threshold pulse, from 10 to 15 ms, while keeping its amplitude constant. Since the calcium bound to TnC at the contraction threshold represents the maximal saturation that will not result in fiber shortening, the difference between the saturation above threshold and at threshold (excess bound calcium; Fig. 7 *A*, Difference) should be regarded as the representation of the calcium that was directly involved in initiating the shortening.

Fig. 7 also presents the simultaneously recorded $\Delta I/I_{850}$ transients both at and above the threshold (Fig. 7 *B*). The trace at the threshold showed a monotonic decline (increase in light intensity), the intrinsic absorbance change of the fiber (Melzer et al., 1986a). Above threshold the movement artifact was superimposed on the monotonic decline of intrinsic fiber absorbance resulting in biphasic transient. The difference of the two records (above threshold-at threshold; Fig. 7 *B*, Difference) is the optical representation of the time course of fiber shortening. It should therefore correlate with the calculated excess bound calcium.

It is expected from the voltage-dependent nature of calcium mobilization from the SR that the latencies of both the excess bound calcium and the optically detected movement should show a clear voltage dependence. Furthermore, the difference between the rise in $[Ca^{2+}]_i$ and the onset of excess bound calcium and/or the contraction should decrease with increasing depolarization due to the faster rate of rise of the calcium transient. On the other hand, the time required for the conformational changes of the contractile proteins and cross-bridge cycling should be independent of the membrane potential. These processes occur after the calcium has bound to TnC and before the fiber actually begins to shorten, thus the difference in the latencies of $\Delta I/I_{850}$ and of the excess bound calcium should be independent of membrane voltage and reflect the time necessary for the activation of thin and thick filaments. It should be noted that the compliant structures within muscle fiber influence the observed delay in shortening; therefore, the value given below is an overestimate of the actual time necessary for the conformational changes to take place (see Discussion).

Fig. 7 *C* presents the latencies calculated from the absorbance records as the function of the latencies of the excess bound calcium. In the measurements using prepulses, the latencies were calculated from the beginning of the first depolarization and not from the beginning of the test pulse. A straight line was fitted through the points using the least-squares method yielding a slope of 1.11 and a *y*-intercept of 8.8 ms. This shows that the two sets of data were closely correlated (the slope was almost unity) and suggests that there was a measurable lag between the calcium binding to TnC and the actual initiation of contraction. Calculating the paired differences of the latencies gave 8.7 ± 0.9 ms (n = 37), a value significantly ($p < 0.01$) greater than zero. In accordance with the above and taking the compliant structures into account (see Discussion), this lag represents an upper estimate of the time necessary for the conformational change of the subunits of troponin, of tropomyosin, and the actomyosin interaction.

Using an actomyosin model to reproduce the time course of isometric force

To extend the analyses presented in the previous sections the measured force was reconstructed on the basis of the calcium transient. Using a least-squares algorithm to minimize the difference between the calculated and measured force transients, the parameters of the steps involved, calcium binding to TnC and the actin–myosin interaction, were also determined.

Fig. 8 demonstrates that the model was capable of predicting the generated force for different calcium concentrations and different levels of mechanical activation by simultaneously fitting five composite calcium transients (Fig. 8 *A*). The depolarizations covered a wide voltage, from −48.6 to −15.9 mV, and $[Ca^{2+}]_i$ range, from 1.6 to 7.1 μM. Fig. 8 *B* presents the measured and fitted force transients superimposed. The obtained value of k_{off} was 70.7 s^{-1} with a corresponding threshold saturation of 0.18. The smallest depolarization was just above threshold, $S_t(max)$ = 0.19, while the largest calcium transient brought TnC close to full, $S_t(max)$ = 0.73, saturation. The parameters obtained from the fit were k_{-2} = 30.4 s^{-1}, k_{-3} = 13.1 s^{-1}, k_{+4} = 18.1 s^{-1}, and M = 3.17. The calculated transients described the latencies and the rising phases of almost all transients remarkably well. The falling phases were, however, less accurately predicted as expected from the work of Stein et al. (1988).

Table 2 summarizes the results from the fits carried out on six fibers. The fits were done as described in connection with Fig. 8 allowing the five parameters (see above) to be fitted. To test if the independent model for the calcium

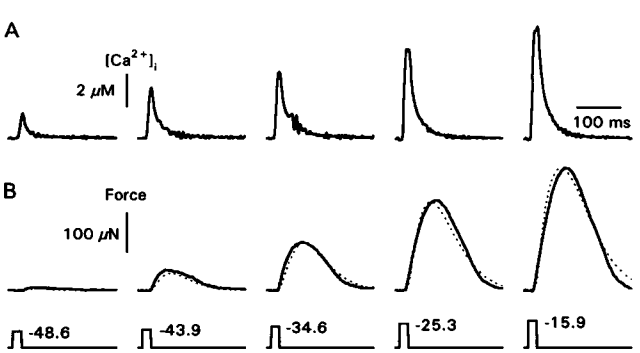

FIGURE 8 Reconstruction of force in a wide voltage range. (*A*) Composite calcium transients evoked by 20-ms-long depolarizing pulses with various amplitudes. The actual time course of membrane potential change is given together with its value during the test depolarization as the lowermost trace in each column. (*B*) The calculated force, dotted traces, superimposed on the measured transients. The least squares fit included all records shown. The parameters of the model that gave the best fit were k_{off} = 91.4 s^{-1}, k_{-2} = 1.78 s^{-1}, k_9 = 56.8 s^{-1}, k_{+4} = 3.53 s^{-1}, M = 4.4. Fiber 274, [APIII] = 401–506 μM, [fura-2] = 20.8–22.7 μM, pl = 90 μm, d = 120 μm, sl = 2.3 μm, T = 11.5°C.

binding to TnC was capable of describing the measured force transients the fits were repeated assuming no interaction between the calcium-specific sites on troponin C. The second row in Table 2 presents the averaged results from these fits. There was no significant change in any of the fitted parameters for the actomyosin interaction; however, both k_{off} and M changed significantly ($p < 0.04$). This decrease was expected, since by losing cooperativity, the model can only compensate for the decrease in calcium binding if the affinity of the sites is increased.

Due to the compliant connections and the relatively low time resolution, these measurements cannot distinguish between different models of the actomyosin interaction. Furthermore, the calculated parameters of the actin and myosin interaction are less meaningful in this oversimplified model. However, the calculated value of k_{off} could be used to determine the other parameters of calcium binding to TnC as it was done in the first section of Results. It should be noted that k_{off} was found rather independent of the actomyosin model used (data not shown, see Discussion) indicating that its value depended more on the measured kinetics of the force transients than on the model chosen.

DISCUSSION

This paper reports calcium and force transients over a wide membrane potential range in voltage clamped amphibian skeletal muscle fibers in a vaseline gap measured simultaneously for the first time. The early events in excitation-contraction coupling were studied and the strength-duration curve analyzed in terms of a hypothesis that a just-detectable contraction corresponds to a constant critical calcium saturation of TnC. We emerged with a quantitative description of the events beginning with an increase in $[Ca^{2+}]_i$ and ending with the generation of force. Our analysis successfully reproduced the time course of force transients and gave estimates for the in vivo calcium binding properties of TnC that agreed with earlier biochemical measurements. The experiments also indicated a voltage-independent delay of 9 ms as an upper limit for the conformational changes in the contractile filaments.

Calcium transients at the contraction threshold

Voltage clamped skeletal muscle fibers need a critical depolarization from the holding potential that depends on the selected pulse duration to produce a just-detectable contraction. This strength-duration relationship was explained in terms of the buildup of a hypothetical activator to a critical level (Adrian et al., 1969). Different groups equated this activator with different physical events in excitation-contraction coupling. Horowicz and Schneider (1981) proposed fixed transfer of intramembrane charge, while Miledi et al. (1983) suggested that a critical level of $[Ca^{2+}]_i$ would correspond to all points on the strength-duration curve. In contrast, when drugs that alter SR calcium release, as caffeine or perchlorate, were used the charge movement and the calcium transient measured at small depolarizations (100 ms pulse duration) of the strength-duration curve were considerably altered, whereas those at large depolarizations and short pulse durations were hardly changed (Csernoch et al., 1987; González and Ríos, 1993). Furthermore, calcium transients were different if measured at different points of the strength-duration curve for just-detectable contraction. The maximal $[Ca^{2+}]_i$ increase was smaller for a 100 ms than for a 10 ms long pulse (Kovács et al., 1987 and Fig. 1 in this paper). These observations led us to propose that the rate constants of the calcium binding to TnC are such that the calcium saturation of TnC would be the same in spite of the different calcium transients.

An alternative possibility explaining the difference in the acquired size of the calcium transients corresponding to different points of the strength-duration curve might arise from diffusional delays. In this framework shorter pulses would need to induce larger calcium transients in order to achieve equal critical $[Ca^{2+}]_i$ at the same calcium-specific sites on TnC. However, the application of a previous analysis of calcium diffusion along the sarcomere (Pizarro et al., 1991) makes such a possibility unlikely unless the TnC binding sites reside in their own, partially isolated, diffusional compartment. We included experiments that make calcium fluxes through such a compartment unlikely. Thus Fig. 3 shows that the predicted values of critical TnC calcium binding were not influenced by conditioning voltage steps that induced a presaturation of the calcium binding sites.

The rate constants of the calcium-troponin C reaction

To determine the calcium binding properties of TnC we assumed, as suggested by Kovács et al. (1987), that its relative saturation reaches a critical level when just-detectable contraction is attained. As demonstrated in Fig. 2 this resulted in two functions relating the three independent parameters, k_{on}, k_{off}, and S_{th}, of calcium binding to TnC. To calculate the actual values of these binding constants one of the above three parameters had to be determined independently. This was done by including k_{off} as one of the fitted parameters in the analysis of force transients (Table 2).

From the two rate constants the off-rate was selected since its values in the literature seem to be less variable (see, e.g., Robertson et al., 1981 for list), even including cardiac isoforms, than values for k_{on}. The value, 78 s^{-1}, obtained for k_{off} from fits to the force transients (Table 2) is in close agreement with those published in the literature (Robertson et al., 1981; Johnson et al., 1981; Rosenfeld et al., 1985). It should be noted that even the value obtained with the independent binding model, 56 s^{-1} (Table 2), is within the limits published earlier.

According to Eq. 8 k_{on} always appears as a multiplicand of the measured $[Ca^{2+}]_i$. Any uncertainty in the detection of

$[Ca^{2+}]_i$ would cause inverse changes in the calculated association rate. That is, if the measured calcium concentration is underestimated, due to possible binding of the dyes to intracellular constituents (Baylor et al., 1986 and Konishi et al., 1988 for APIII and fura-2, respectively), the calculated association rate and, consequently, the association constant would be overestimated. On the other hand, any uncertainties in $[Ca^{2+}]_i$ are compensated for with changes in k_{on}. This also establishes the fact that the obtained values of k_{off} and S_{th} are independent of the scaling of $[Ca^{2+}]_i$.

The question, however, is whether the selection of the actomyosin model influenced the calculated value of k_{off}. In our earlier calculations (e.g., Kovács et al., 1995) a more elaborate model of Dantzig et al. (1992) was used that included, among others, the binding of substrates and a distortion-dependent transition. In this paper we adopted a much simpler model. Nevertheless, the obtained k_{off} was essentially independent of the model used, 78 s^{-1} in these calculations and 85 s^{-1} in Kovács et al. (1995) using the above mentioned model, showing that it most likely represents the true value of k_{off}.

Validity of the models used to calculate the calcium activation of the thin filament

To calculate the calcium binding to TnC a cooperative binding reaction scheme was used (S1) since several papers have been published on thin filament cooperativity (e.g., Rosenfeld et al., 1985) even showing that binding of calcium to one of the calcium specific sites can not trigger contraction alone (Sheng et al., 1990). Stein et al. (1988) even argued that cooperative interaction gave better fits to the force transient in frogs than did the non-cooperative. Nevertheless, as shown in Fig. 1, the independent binding model gave a similar time course if the threshold saturation of TnC was assumed to be the same.

Earlier reports on calcium regulation of skeletal muscle activation (Hill, 1983) assumed a change in the affinity of TnC for calcium upon the association of actin with myosin. This was incorporated into the model by changing k_{off} proportionally with the association of actin to myosin. Although the obtained change in affinity 3.6 and 5.6 (parameter M in Table 2) was smaller than that used by Hill (1983) it was significantly greater than 1, suggesting that such change is present under in vivo conditions.

Neighboring tropomyosin molecules were also assumed to interact and this interaction was proposed to account for, or part of, the cooperativity seen with myosin subfragment-1 and regulated actin (Wegner, 1979; Hill, 1983). Following the line of reasoning given by Hill (1983) the interaction of neighboring tropomyosins would result in a higher interaction free energy (a greater negative value) if the two molecules were in the same state. Assuming only two states, one that allows and one that blocks the actomyosin interaction, the ratio of the molecules in the two states calculates to ~0.18. This corresponds to $e^{-1.7}$, during the calculations e^{-2} was used throughout (using an integer as the power greatly reduced the calculation time).

The time required for the activation of the contractile filaments

The present theory of the regulation of skeletal muscle contraction, the inhibition of actomyosin interaction via troponin and tropomyosin, predicts that after the binding of calcium to the regulatory domain of troponin (subunit C), several conformational changes must take place before actual shortening can begin.

Diffraction studies have revealed that certain reflections that are associated with the thin filaments occur in fibers stretched beyond filament overlap (Kress et al., 1986) demonstrating that structural changes take place within the thin filaments without any interaction between actin and myosin. In the report of Kress et al. (1986), where the time resolution is the best, the difference between the change in diffraction and the onset of contraction is ~5 ms (value read from Fig. 3 of that paper) which is in good agreement with our estimation of 9 ms. The reason for the slightly higher value obtained in this study might reflect that our value includes the conformational change of TnC as well, while those from diffraction studies probably report the time after the movement of tropomyosin.

Compliant structures and connections might interfere with the estimation of delays in force development and rise. As an example, the compliant nature of the thin filament might account for some, or much, of the delays observed in x-ray diffraction (Huxley et al., 1994). A series of experiments were, therefore, preformed to estimate the compliance of our system (we are not aware of any previous estimates of the compliance of the single vaseline gap system). Under essentially the same conditions the tendon had a compliance of 1.5×10^{-2} m/N, the fiber and the tendon together 3.4×10^{-2} m/N, and the full system 6.1×10^{-2} m/N. As expected, these values are higher than the corresponding data published for skinned fibers attached to steel hooks (e.g., Higuchi et al., 1995). To minimize the error resulting from the compliance of the connection we used the optical signal on the fiber as an indicator of movement. Although its time course was too complex to simply equate with that of force the onset was reliably detected. This method, although eliminating problems arising from compliant connections, could not reduce any delay originating from the compliant filaments rendering the obtained value, 8.7 ms, an upper estimate for the time of the interactions in the contractile filaments.

It should be noted, however, that although the latency of contraction was always longer than the latency of reaching threshold saturation of TnC, the obtained differences varied between 2 and 15 ms (see Fig. 7 *C*). This renders the calculated average value of the difference less meaningful, despite the small (1 ms) standard error of the mean. The scatter was, at least in part, due to the imperfect estimation

of the threshold saturation, e.g., if the threshold saturation was underestimated in a given fiber the difference in latencies was overestimated.

The authors are indebted to Dr. C. L.-H. Huang for carefully reading and discussing the manuscript, to Dr. G. J. M. Stienen for helpful comments, and to R. Őri for skilled technical assistance.

This work was sponsored by Hungarian OTKA Grants T016957 and F5467, and the Muscular Dystrophy Association.

REFERENCES

Adrian, R. H., W. K. Chandler, and A. L. Hodgkin. 1969. The kinetics of mechanical activation in frog muscle. *J. Physiol.* 204:207–230.

Baylor, S. M., S. Hollingworth, C. S. Hui, and M. E. Quinta-Ferreira. 1986. Properties of the metallochromic dyes arsenazo III, antipyrylazo III and azo 1 in frog skeletal muscle fibers at rest. *J. Physiol.* 377:89–141.

Claflin, D. R., D. L. Morgan, D. G. Stephenson, and F. J. Julian. 1994. The intracellular Ca^{2+} transients and tension in frog skeletal muscle fibers measured with high temporal resolution. *J. Physiol.* 475:319–325.

Close, R. I. 1981. Activation delays in frog twitch muscle fibers. *J. Physiol.* 313:81–100.

Csernoch, L., V. Jacquemond, and M. F. Schneider. 1993. Microinjection of strong calcium buffers suppresses the peak of calcium release in frog skeletal muscle fibers. *J. Gen. Physiol.* 101:297–333.

Csernoch, L., L. Kovács, and G. Szűcs. 1987. Perchlorate and the relationship between charge movement and contractile activation in frog skeletal muscle fibers. *J. Physiol.* 390:213–227.

Csernoch, L., G. Pizarro, I. Uribe, M. Rodríguez, and E. Ríos. 1991. Interfering with calcium release suppresses $I\gamma$, the "hump" component of intramembranous charge movement in skeletal muscle. *J. Gen. Physiol.* 97:845–884.

Csernoch, L., P. Szentesi, G. Szűcs, and L. Kovács. 1994. Time course of fiber shortening and its temporal correlation to calcium binding to troponin C in skeletal muscle. *J. Muscle Res. Cell Motil.* 15:174*a*. (Abstr.).

Dantzig, J. A., Y. E. Goldman, N. C. Millar, J. Lacktis, and E. Homsher. 1992. Reversal of the cross-bridge force-generating transition by photogeneration of phosphate in rabbit psoas muscle fibers. *J. Physiol.* 451:247–278.

Dobrunz, L. E., P. H. Backx, and D. T. Yue. 1995. Steady-state $[Ca^{2+}]_i$-force relationship in intact twitching cardiac muscle: direct evidence for modulation by isoproterenol and EMD 53998. *Biophys. J.* 69:189–201.

Geeves, M. A., and S. S. Lehrer. 1994. Dynamics of the muscle thin filament regulatory switch: the size of the cooperative unit. *Biophys. J.* 67:273–282.

Goldman, Y. E. 1987. Kinetics of the actomyosin ATPase in muscle fibers. *Annu. Rev. Physiol.* 49:637–654.

Gomolla, M., G. Gottschalk, and H. C. Lüttgau. 1983. Perchlorate-induced alteration in electrical and mechanical parameters of frog skeletal muscle fibers. *J. Physiol.* 343:197–214.

González, A., and E. Ríos. 1993. Perchlorate enhances transmission in skeletal muscle excitation-contraction coupling. *J. Gen. Physiol.* 102: 373–421.

Güth, K., and J. D. Potter. 1987. Effect of rigor and cycling cross-bridges on the structure of troponin C and Ca^{2+} affinity of the Ca^{2+}-specific regulatory sites in skinned rabbit psoas fibers. *J. Biol. Chem.* 262: 13627–13635.

Higuchi, H., T. Yanagida, and Y. E. Goldman. 1995. Compliance of thin filaments in skinned fibers of rabbit skeletal muscle. *Biophys. J.* 69: 1000–1010.

Hill, T. L. 1983. Two elementary models for the regulation of skeletal muscle contraction by calcium. *Biophys. J.* 44:383–396.

Horowicz, P., and M. F. Schneider. 1981. Membrane charge moved at contraction thresholds in skeletal muscle fibers. *J. Physiol.* 277: 483–506.

Huxley, H. E., A. Stewart, H. Sosa, and T. Irving. 1994. X-ray diffraction measurements of the extensibility of actin and myosin filaments in contracting muscle. *Biophys. J.* 67:2411–2421.

Johnson, M. L., and L. M. Faunt. 1992. Parameter estimation by least-squares methods. *In* Numerical Computer Methods. L. Brand and M. L. Johnson, editors. Academic Press, San Diego. 1–37.

Johnson, J. D., D. E. Robinson, S. P. Robertson, A. Schwartz, and J. D. Potter. 1981. Ca^{2+} exchange with troponin and the regulation of muscle contraction. *In* Regulation of Muscle Contraction: Excitation-Contraction Coupling. A. D. Grinnell and M. A. B. Brazier, editors. Academic Press, New York. 241–257.

Klein, M. G., B. J. Simon, G. Szűcs, and M. F. Schneider. 1988. Simultaneous recording of calcium transients in skeletal muscle using high and low affinity calcium indicators. *Biophys. J.* 55:971–988.

Konishi, M., A. Olson, S. Hollingworth, and S. M. Baylor. 1988. Myoplasmic binding of Fura-2 investigated by steady-state fluorescence and absorbance measurements. *Biophys. J.* 54:1089–1104.

Kovács, L., P. Szentesi, and L. Csernoch. 1995. Kinetic comparison of isometric tension and intracellular calcium concentration changes in frog skeletal muscle fibers. *J. Physiol.* 487:159.

Kovács, L., G. Szűcs, and L. Csernoch. 1987. Calcium transients and calcium binding to troponin at the contraction threshold in skeletal muscle. *Biophys. J.* 51:521–526.

Kress, M., H. E. Huxley, A. R. Faruqi, and J. Hendrix. 1986. Structural changes during activation of frog muscle studied by time-resolved X-ray diffraction. *J. Mol. Biol.* 188:325–342.

Melzer, W., E. Ríos, and M. F. Schneider. 1986a. The removal of myoplasmic free calcium following calcium release in frog skeletal muscle. *J. Physiol.* 372:261–292.

Melzer, W., M. F. Schneider, B. J. Simon, and G. Szűcs. 1986b. Intramembrane charge movement and calcium release in frog skeletal muscle. *J. Physiol.* 373:481–511.

Miledi, R., I. Parker, and P. H. Zhu. 1983. Calcium transients studied under voltage-clamp control in frog twitch muscle fibers. *J. Physiol.* 340: 649–680.

Pizarro, G., L. Csernoch, I. Uribe, M. Rodríguez, and E. Ríos. 1991. The relationship between Q_γ and Ca release from the sarcoplasmic reticulum in skeletal muscle. *J. Gen. Physiol.* 97:913–947.

Robertson, S. P., J. D. Johnson, and J. D. Potter. 1981. The time-course of Ca^{2+} exchange with calmodulin, troponin, parvalbumin, and myosin in response to transient increases in Ca^{2+}. *Biophys. J.* 34:559–569.

Rosenfeld, S. S., and E. W. Taylor. 1985. Kinetic studies of calcium binding to regulatory complexes from skeletal muscle. *J. Biol. Chem.* 260:252–261.

Sárközi, S., P. Szentesi, I. Jona, and L. Csernoch. 1996. Effects of cardiac glycosides on excitation-contraction coupling in frog skeletal muscle fibers. *J. Physiol.* 495:611–626.

Sheng, Z., W. L. Strauss, J.-M. Francois, and J. D. Potter. 1990. Evidence that both Ca^{2+} specific sites of skeletal muscle TnC are required for full activity. *J. Biol. Chem.* 265:21554–21560.

Stein, R. B., J. Bobet, M. N. Oguztoreli, and M. Fryer. 1988. The kinetics relating calcium and force in skeletal muscle. *Biophys. J.* 54:705–717.

Stienen, G. J. M., R. Zaremba, and G. Elzinga. 1995. ATP utilization for calcium uptake and force production in skinned muscle fibers of *Xenopus laevis*. *J. Physiol.* 482:109–122.

Tregear, R. T., and S. B. Marston. 1979. The crossbridge theory. *Annu. Rev. Physiol.* 41:723–736.

Wegner, A. 1979. Equilibrium of the actin-tropomyosin interaction. *J. Mol. Biol.* 131:839–853.